ELSEVIER

International Journal of Solids and Structures 41 (2004) 1139–1155

INTERNATIONAL JOURNAL OF SOLIDS and STRUCTURES

www.elsevier.com/locate/ijsolstr

On the thermo-mechanical coupling in austenite–martensite phase transformation related to the quenching process

Eduardo Prieto Silva [a], Pedro Manuel Calas Lopes Pacheco [b,*], Marcelo Amorim Savi [c]

[a] *Volkswagen South America, Truck and Bus, Development, Certification and Test, DCT Chassis, 27.501.970, Resende, RJ, Brazil*
[b] *CEFET/RJ, Centro Federal de Educação Tecnológica Celso Suckow da Fonseca, Department of Mechanical Engineering, Av. Maracana 229, 20.271.110, Rio de Janeiro, RJ, Brazil*
[c] *Universidade Federal do Rio de Janeiro, COPPE—Department of Mechanical Engineering, Caixa Postal 68.503, 21.945.970, Rio de Janeiro, RJ, Brazil*

Received 13 June 2002; received in revised form 14 July 2003

Abstract

The present contribution considers modeling and simulation of the quenching process, presenting an anisothermal model formulated within the framework of continuum mechanics and the thermodynamics of irreversible processes. The energy equation thermo-mechanical coupling terms due to internal and thermal couplings are exploited. In order to analyze the importance of these terms, three different models are considered. The first one is an uncoupled model in the sense that these terms are neglected, corresponding to the rigid body energy equation. In second model, these couplings are represented through the incorporation of a source term in the energy equation associated with the latent heat released during the austenite–martensite phase transformation. Finally, the third model considers all thermo-mechanical coupling terms of the proposed model. Progressive induction hardening of a long cylindrical body is considered as an application of the proposed general formulation. Numerical simulations analyze the effect of the thermo-mechanical coupling terms, comparing the three proposed models.

Keywords: Quenching; Phase transformation; Thermo-mechanical coupling; Modeling

1. Introduction

Quenching is a commonly used heat treatment process employed to control the mechanical properties of steels. In brief, quenching consists of raising the temperature of the steel above a certain critical temperature, called austenitizing temperature, holding it at that temperature for a fixed time, and then rapidly cooling it in a suitable medium to room temperature. The resulting microstructures formed from quenching

* Corresponding author. Tel./fax: +55-2125694495.
E-mail addresses: eduardo.silva3@volkswagen.com.br (E.P. Silva), calas@cefet-rj.br (P.M.C.L. Pacheco), savi@ufrj.br (M.A. Savi).

0020-7683/$ - see front matter © 2003 Elsevier Ltd. All rights reserved.
doi:10.1016/j.ijsolstr.2003.09.049

(ferrite, pearlite, bainite and martensite) depend on cooling rate and on steel characteristics, which are normally expressed by the Continuous Cooling Transformation (CCT) diagram.

The formation of martensite can be induced if the steel is austenitized and then cooled at a sufficiently high rate in order to avoid the formation of ferrite, pearlite and bainite. The volumetric expansion associated with the formation of martensite combined with large temperature gradients and non-uniform cooling promotes high residual stresses that can induce distortion or even cracking in quenched steels. Therefore, the prediction of such stresses is very important being a rather difficult task. Many works are devoted to the prediction of residual stresses in quenched steels (Denis, 1996; Denis et al., 1985, 1987, 1992, 1999; Fernandes et al., 1985, 1986; Woodard et al., 1999; Sjöström, 1985, 1994; Sen et al., 2000), however, the proposed models are not generic and are usually applicable to simple geometries.

Phenomenological aspects of quenching involve couplings among different physical processes and its description is unusually complex. Basically, three couplings are essential: thermal, phase transformation and mechanical phenomena. Pacheco et al. (2001) propose a constitutive model to describe the thermo-mechanical behavior related to the quenching process considering the austenite–martensite phase transformation. This anisothermal model is formulated within the framework of continuum mechanics and the thermodynamics of irreversible processes. One of the advantages of this formulation is the possibility to identify couplings, estimating the effect of each one on the process. The cited reference considers a numerical procedure based on the operator split technique associated with an iterative numerical scheme in order to deal with non-linearities in the formulation. With this assumption, the coupled governing equations are solved from four uncoupled problems. The proposed general formulation is applied to the progressive induction hardening of steel cylinders. In the cited reference, numerical results are carried out neglecting energy equation thermo-mechanical coupling terms associated with internal and thermal couplings.

The present contribution revisits this constitutive model exploiting the thermo-mechanical coupling terms in the energy equation considering austenite–martensite phase transformation process. These terms may become important on the description of quenching process and the analysis of their influence is not completely reported in literature. Sjöström (1985), for example, says that thermo-mechanical coupling terms in the energy equation are essential in the modeling of quenching process. Habraken and Bourdouxhe (1992) and Woodard et al. (1999) present a finite element analysis considering energy equation couplings as a latent heat, showing that it is an essential effect to be considered in the modeling of quenching. Levitas (1997, 1998, 2000) and Idesman et al. (1997, 2000) made important contributions to the study of thermo-mechanical aspects of phase transformation in elastoplastic materials.

In this article, numerical simulations establish a comparison among three different models: *Uncoupled*, which does not include energy equation coupling terms; *Latent heat*, with a source term in the energy equation associated with the latent heat released during the martensitic phase transformation; and *Coupled*, that considers all coupling terms in the proposed model.

2. Constitutive model

The thermodynamic state of a solid is completely defined by the knowledge of the state variables. Constitutive equations may be formulated within the framework of continuum mechanics and the thermodynamics of irreversible processes, by considering thermodynamic forces, defined from the Helmholtz free energy, ψ, and thermodynamic fluxes, defined from the pseudo-potential of dissipation, ϕ (Pacheco et al., 2001).

The quenching model here proposed allows one to identify different coupling phenomena, estimating the effect of each one on the process. With this aim, a Helmholtz free energy is proposed as a function of

observable variables, total strain, ε_{ij}, and temperature, T. Moreover, internal variables are considered: plastic strain, $\varepsilon^{\mathrm{p}}_{ij}$, volumetric fraction of martensitic phase, β, and another set of variables associated with the phase transformation, hardening and other effects as damage. Here, this set considers just a variable related to kinematic hardening, α_{ij}. Therefore, the following free energy is considered, presented in indicial notation where summation convention is evoked (Eringen, 1967):

$$\rho\psi(\varepsilon_{ij},\varepsilon^{\mathrm{p}}_{ij},\alpha_{ij},\beta,T)=W(\varepsilon_{ij},\varepsilon^{\mathrm{p}}_{ij},\alpha_{ij},\beta,T)=W_{\mathrm{e}}(\varepsilon_{ij}-\varepsilon^{\mathrm{p}}_{ij},\beta,T)+W_{\alpha}(\alpha_{ij})+W_{\beta}(\beta)-W_{\mathrm{T}}(T) \tag{1}$$

where ρ is the material density. The elastic strain is defined as follows:

$$\varepsilon^{\mathrm{e}}_{ij}=\varepsilon_{ij}-\varepsilon^{\mathrm{p}}_{ij}-\alpha_{\mathrm{T}}(T-T_0)\delta_{ij}-\gamma\beta\delta_{ij}-(3/2)\kappa\sigma^{\mathrm{d}}_{ij}\beta(2-\beta) \tag{2}$$

In the right hand of this expression, the first term is the total strain while the second is related to plastic strain. The third term, $\alpha_{\mathrm{T}}(T-T_0)\delta_{ij}$, is associated with thermal expansion. The parameter α_{T} is the coefficient of linear thermal expansion, T_0 is a reference temperature and δ_{ij} is the Kronecker delta. The fourth term, $\gamma\beta\delta_{ij}$, is related to volumetric expansion associated with phase transformation from austenite to martensite. Therefore, when part of a material experiences phase transformation, there is an increment of volumetric strain, proportional to γ, a material property related to the total expansion associated with martensitic transformation. Finally, the last term, $(3/2)\kappa\sigma^{\mathrm{d}}_{ij}\beta(2-\beta)$, is denoted as transformation plasticity strain, being the result of several physical mechanisms (Denis et al., 1985; Sjöström, 1985; Cherkaoui, 2002). This behavior is related to localized plastic strain promoted by the martensitic transformation. In this term, the deviatoric stress component is defined by $\sigma^{\mathrm{d}}_{ij}=\sigma_{ij}-\delta_{ij}(\sigma_{kk}/3)$, with σ_{ij} being the stress tensor component. Moreover, κ is a material parameter. It should be emphasized that this strain may be related to stress states that are inside the yield surface.

With these assumptions, energy functions may be expressed by,

$$W_{\alpha}(\alpha_{ij})=\tfrac{1}{2}H_{ijkl}\alpha_{ij}\alpha_{kl} \tag{3}$$

$$W_{\mathrm{T}}(T)=\rho\int_{T_0}^{T}C_1\log(\xi)\,\mathrm{d}\xi+\frac{\rho}{2}C_2T^2 \tag{4}$$

$$W_{\beta}(\beta)=I_{\beta}(\beta) \tag{5}$$

$$\begin{aligned}W_{\mathrm{e}}(\varepsilon_{ij}-\varepsilon^{\mathrm{p}}_{ij},\beta,T)=\Phi_{ijpq}E_{pqkl}\left[\frac{1}{2}(\varepsilon_{ij}-\varepsilon^{\mathrm{p}}_{ij})(\varepsilon_{kl}-\varepsilon^{\mathrm{p}}_{kl})-(\alpha_{\mathrm{T}}(T-T_0)+\gamma\beta)(\varepsilon_{ij}-\varepsilon^{\mathrm{p}}_{ij})\delta_{kl}\right]\\ +\frac{\Phi_{ijpq}E_{pqkk}\left[\frac{1}{2}\kappa\beta(2-\beta)\right]\Phi_{aaef}E_{efrs}\left[\frac{1}{2}(\varepsilon_{ij}-\varepsilon^{\mathrm{p}}_{ij})(\varepsilon_{rs}-\varepsilon^{\mathrm{p}}_{rs})-(\alpha_{\mathrm{T}}(T-T_0)+\gamma\beta)(\varepsilon_{ij}-\varepsilon^{\mathrm{p}}_{ij})\delta_{rs}\right]}{\left(1-\Phi_{bbcd}E_{cdgg}\left[\frac{1}{2}\kappa\beta(2-\beta)\right]\right)}\end{aligned} \tag{6}$$

The components E_{ijkl} and H_{ijkl} are associated with elastic and hardening tensors, respectively; C_1 and C_2 are positive constants. Auxiliary tensors are also defined in order to simplify the previous expression:

$$C_{ijpq}=\delta_{pi}\delta_{qj}+\tfrac{3}{2}E_{ijpq}\kappa\beta(2-\beta) \tag{7}$$

$$\Phi_{ijpq}=C^{-1}_{ijpq} \tag{8}$$

Tensor component Φ_{ijpq} is associated with the inverse of C_{ijpq} and $I_{\beta}(\beta)$ is the indicator function related to the convex set $C_{\beta}=\{\beta|0\leqslant\beta\leqslant1\}$ (Rockafellar, 1970).

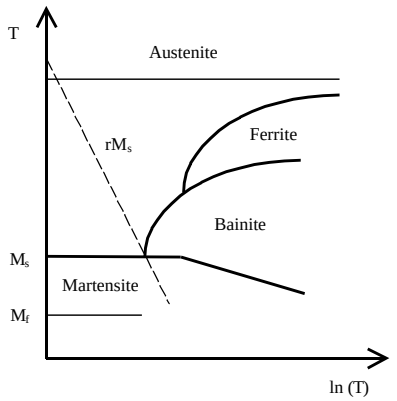

Fig. 1. CCT diagram and the critical cooling rate rM_s.

The austenite–martensite phase transformation is described with the aid of the following condition:

$$\varsigma_{A\to M}(\dot{T},T)=\Gamma(-\dot{T}-rMs)\Gamma(M_s-T)\Gamma(T-M_f) \tag{9}$$

where rM_s is the critical cooling rate for the martensite formation, defined from the CCT diagram, Fig. 1; $\dot{T}$ is the cooling rate. Moreover, $\Gamma(x)$ is the Heaviside function defined as follows (Wang et al., 1997):

$$\Gamma(x)=\begin{cases}1, & x\geqslant 0\\ 0, & x<0\end{cases} \tag{10}$$

Therefore, the kinetics of martensitic phase transformation may be expressed by

$$\beta=\beta(T,\dot{T})=\varsigma_{A\to M}\beta^m \tag{11}$$

where β^m is defined from the equation proposed by Koistinen and Marburger (1959):

$$\beta^m=1-\exp[-k(M_s-T)] \tag{12}$$

here, k is a material constant. M_s is the temperature where martensite starts to form in a stress-free state and M_f is the temperature where martensite finishes its formation in a stress-free state.

Thermodynamics forces $(\sigma_{ij},P_{ij},X_{ij},B^{\beta},s)$, associated with state variables $(\varepsilon_{ij},\varepsilon^{p}_{ij},\alpha_{ij},\beta,T)$, are defined as follows:

$$\begin{aligned}\sigma_{ij}&=\frac{\partial W}{\partial\varepsilon_{ij}}\\ &=\Phi_{ijpq}E_{pqkl}\left[\varepsilon_{kl}-\varepsilon^{p}_{kl}-(\alpha_T(T-T_0)+\gamma\beta)\delta_{kl}\right]+\Phi_{ijpq}E_{pqkk}\left[\frac{1}{2}\kappa\beta(2-\beta)\right]\\ &\quad\times\left\{\frac{\Phi_{aaef}E_{efrs}\left[\varepsilon_{rs}-\varepsilon^{p}_{rs}-(\alpha_T(T-T_0)+\gamma\beta)\delta_{rs}\right]}{1-\Phi_{bbcd}E_{cdgg}\left[\frac{1}{2}\kappa\beta(2-\beta)\right]}\right\}\end{aligned} \tag{13}$$

$$P_{ij}=-\frac{\partial W}{\partial\varepsilon^{p}_{ij}}=\sigma_{ij} \tag{14}$$

$$X_{ij} = \frac{\partial W}{\partial \alpha_{ij}} = H_{ijkl}\alpha_{kl} \tag{15}$$

$$s = -\frac{1}{\rho}\frac{\partial W}{\partial T} \tag{16}$$

$$B^{\beta} = -\frac{\partial W}{\partial \beta} = -\left(\frac{\partial W_{\mathrm{e}}}{\partial \beta} + Z\right) \tag{17a}$$

$$B^{\beta} = E_{pqkl}(\varepsilon_{ij} - \varepsilon_{ij}^{\mathrm{p}})\left\{A_{ijpqkl} + \frac{E_{efrs}\delta_{kl}}{\Xi}\left[B_{ijpqefrs} + M_{ijpqefrs} + \frac{N_{ijpqefrs}}{\Xi}\right]\right\} - Z \tag{17b}$$

where

$$\Xi = 1 - \Phi_{zzhn}E_{hnxx}\left[\frac{1}{2}\kappa\beta(2-\beta)\right] \tag{18}$$

Again, auxiliary tensors are defined in order to simplify the expressions presented before:

$$A_{ijpqkl} = \frac{\partial \Phi_{ijpq}}{\partial \beta}\left\{(\alpha_{\mathrm{T}}(T - T_0) + \gamma\beta)\delta_{kl} - \frac{1}{2}(\varepsilon_{kl} - \varepsilon_{kl}^{\mathrm{p}})\right\} + \Phi_{ijpq}\gamma\delta_{kl} \tag{19}$$

$$B_{ijpqefrs} = \left[\frac{1}{2}\kappa\beta(2-\beta)\right]\left(\frac{\partial \Phi_{ijpq}}{\partial \beta}\Phi_{aaef} + \Phi_{ijpq}\frac{\partial \Phi_{aaef}}{\partial \beta}\right)\left\{(\alpha_{\mathrm{T}}(T - T_0) + \gamma\beta)\delta_{rs} - \frac{1}{2}(\varepsilon_{rs} - \varepsilon_{rs}^{\mathrm{p}})\right\} \tag{20}$$

$$M_{ijpqefrs} = \Phi_{ijpq}\Phi_{aaef}\left\{\kappa(1-\beta)\left((\alpha_{\mathrm{T}}(T - T_0) + \gamma\beta)\delta_{rs} - \frac{1}{2}(\varepsilon_{rs} - \varepsilon_{rs}^{\mathrm{p}})\right) + \gamma\left[\frac{1}{2}\kappa\beta(2-\beta)\right]\delta_{rs}\right\} \tag{21}$$

$$\begin{aligned} N_{ijpqefrs} = {} & \Phi_{ijpq}\left[\frac{1}{2}\kappa\beta(2-\beta)\right]\Phi_{aaef}\left\{E_{cdgg}\left(\frac{\partial \Phi_{bbcd}}{\partial \beta}\left[\frac{1}{2}\kappa\beta(2-\beta)\right] + \Phi_{bbcd}\kappa(1-\beta) - \right)\right\} \\ & \times \left\{(\alpha_{\mathrm{T}}(T - T_0) + \gamma\beta)\delta_{rs} - \frac{1}{2}(\varepsilon_{rs} - \varepsilon_{rs}^{\mathrm{p}})\right\} \end{aligned} \tag{22}$$

$Z \in \partial_{\beta} I_{\beta}(\beta)$ is the sub-differential of the indicator function I_{β} (Rockafellar, 1970).

In order to describe dissipation processes, it is necessary to introduce a potential of dissipation $\phi(\dot{\varepsilon}_{ij}^{\mathrm{p}}, \dot{\alpha}_{ij}, \dot{\beta}, q_i)$, which can be split into two parts: $\phi(\dot{\varepsilon}_{ij}^{\mathrm{p}}, \dot{\alpha}_{ij}, \dot{\beta}, q_i) = \phi_1(\dot{\varepsilon}_{ij}^{\mathrm{p}}, \dot{\alpha}_{ij}, \dot{\beta}) + \phi_2(q_i)$. This potential can be written through its dual $\phi^*(P_{ij}, X_{ij}, B^{\beta}, g_i) = \phi_1^*(P_{ij}, X_{ij}, B^{\beta}) + \phi_2^*(g_i)$, as follows:

$$\begin{cases} \phi_1^* = I_{\mathrm{f}}^*(P_{ij}, X_{ij}) + \varsigma_{\mathrm{A}\to\mathrm{M}}\dot{\beta}^m B^{\beta} \\ \phi_2^* = \frac{T}{2}\Lambda g_i g_i \end{cases} \tag{23}$$

where $g_i = (1/T)\partial T/\partial x_i$ and Λ is the coefficient of thermal conductivity which is a function of temperature; $I_{\mathrm{f}}^*(P_{ij}, X_{ij})$ is the indicator function associated with elastic domain, related to the *von Mises* criterion (Lemaitre and Chaboche, 1990),

$$f(P_{ij}, X_{ij}) = \left[\frac{3}{2}(P_{ij}^{\mathrm{d}} - X_{ij}^{\mathrm{d}})(P_{ij}^{\mathrm{d}} - X_{ij}^{\mathrm{d}})\right]^{1/2} - \sigma_{\mathrm{Y}} \leqslant 0 \tag{24}$$

σ_{Y} is the material yield stress, $X_{ij}^{\mathrm{d}} = X_{ij} - \delta_{ij}(X_{kk}/3)$ and $P_{ij}^{\mathrm{d}} = \sigma_{ij}^{\mathrm{d}}$. A set of evolution laws obtained from ϕ^* characterizes dissipative processes,

$$\dot{\varepsilon}_{ij}^{\mathrm{p}} \in \partial_{P_{ij}} I_{\mathrm{f}}^*(P_{ij}, X_{ij}) = \lambda\ \mathrm{sign}\,(\sigma_{ij} - H_{ijkl}\alpha_{kl}) \tag{25}$$

$$\dot{\alpha}_{ij} \in -\partial_{X_{ij}} I_{\mathrm{f}}^{*}(\sigma_{ij}, X_{ij}) = \dot{\varepsilon}_{ij}^{\mathrm{p}} \tag{26}$$

$$\dot{\beta} = \frac{\partial \phi^{*}}{\partial B^{\beta}} = \varsigma_{\mathrm{A}\to\mathrm{M}} \dot{\beta}^{m} \tag{27}$$

$$q_i = -\frac{\partial \phi^{*}}{\partial g_i} = -\Lambda T \quad g_i = -\Lambda \frac{\partial T}{\partial x_i} \tag{28}$$

where $\mathrm{sign}(x) = x/|x|$; q_i is related to heat flux vector and λ is the plastic multiplier from the classical theory of plasticity (Lemaitre and Chaboche, 1990).

Assuming a specific heat as $c = -(T/\rho)\partial^2 W_{\mathrm{T}}/\partial T^2$ and the set of constitutive equations (13–17, 25–28), the energy equation can be written as

$$\frac{\partial}{\partial x_i}\left(\Lambda \frac{\partial T}{\partial x_i}\right) - \rho c \dot{T} = -a_{\mathrm{I}} - a_{\mathrm{T}} \tag{29}$$

where,

$$a_{\mathrm{I}} = \sigma_{ij}\dot{\varepsilon}_{ij}^{\mathrm{p}} - X_{ij}\dot{\alpha}_{ij} + B^{\beta}\dot{\beta} \tag{30a}$$

$$a_{\mathrm{T}} = T\left(\frac{\partial \sigma_{ij}}{\partial T}(\dot{\varepsilon}_{ij} - \dot{\varepsilon}_{ij}^{\mathrm{p}}) + \frac{\partial X_{ij}}{\partial T}\dot{\alpha}_{ij} - \frac{\partial B^{\beta}}{\partial T}\dot{\beta}\right) \tag{30b}$$

The term a_{I} is denoted as internal coupling and is always positive. It has a role in Eq. (29) similar to a heat source in the classical energy equation (heat equation) for rigid bodies. The term a_{T} denotes the thermal coupling and can be either positive or negative.

With these assumptions, the set of constitutive equations formed by (13–17, 25–28) verify the inequality established by the second law of thermodynamics which can be expanded in a local form as:

$$\begin{cases} d_1 = \sigma_{ij}\dot{\varepsilon}_{ij}^{\mathrm{p}} - X_{ij}\dot{\alpha}_{ij} + B^{\beta}\dot{\beta} \geqslant 0 \\ d_2 = -(q_i g_i) \geqslant 0 \end{cases} \tag{31}$$

The term d_1 represents mechanical dissipation while d_2 the thermal dissipation.

It should be pointed out that the coupling term $Z\dot{\beta}$ from the term $B^{\beta}\dot{\beta}$ (Eq. (30a)), always vanishes. Notice that if $T > M_{\mathrm{s}}$ and $T < M_{\mathrm{f}}$, then $\dot{\beta} = 0$ and the term is zero. On the other hand, if $M_{\mathrm{s}} \geqslant T \geqslant M_{\mathrm{f}}$, $\dot{\beta} \neq 0$. However, from the definition of the indicator function, $I_{\beta} = 0$, and therefore, the coupling term must be zero again. For the same reasons, $\frac{\partial Z}{\partial T}\dot{\beta}$ always vanishes (Eq. (30b)).

In metal forming, the thermo-mechanical coupling is usually taken into account by an empirical constant called the heat conversion factor, χ, which represents the part of the plastic power transformed into heat (Pacheco, 1994):

$$\chi = \frac{a_{\mathrm{I}} + a_{\mathrm{T}}}{\sigma_{ij}\dot{\varepsilon}_{ij}^{\mathrm{p}}} \tag{32}$$

Some authors consider the thermo-mechanical coupling effect related to phase transformation as a latent heat released during phase transformation. (Denis et al., 1987; Denis et al., 1999; Woodard et al., 1999; Sjöström, 1994). Therefore, the latent heat released during phase transformation may be described by an internal heat source term:

$$\dot{Q} = \Delta H_{\mathrm{m}} \dot{\beta} \tag{33}$$

where ΔH_{m} is the enthalpy variation during austenite–martensite transformation (Woodard et al., 1999).

3. Cylindrical bodies

This contribution considers long cylindrical bodies as an application of the proposed general formulation. Other references present different analyses of this problem (Pacheco et al., 1997; Camarão et al., 2000). With this assumption, heat transfer analysis may be reduced to a one-dimensional problem. Also, plane stress or plane strain state can be assumed. Under these assumptions, only radial, r, circumferential, θ, and longitudinal, z, components need to be considered. In brief, it is important to notice that tensor quantities may be replaced by scalar or vector quantities. As examples, one could mention: E_{ijkl} replaced by E; H_{ijkl} replaced by H; σ_{ij} replaced by σ_i $(\sigma_{\mathrm{r}}, \sigma_\theta, \sigma_z)$. A detailed description of these simplifications could be found in Pacheco et al. (2001).

The numerical procedure here proposed is based on the operator split technique (Ortiz et al., 1983; Pacheco, 1994) associated with an iterative numerical scheme in order to deal with non-linearities in the formulation. With this assumption, coupled governing equations are solved from four uncoupled problems, allowing the use of classical numerical procedures: thermal, phase transformation, thermo-elastic and elastoplastic.

Thermal problem—Comprises a radial conduction problem with convection. Material properties depend on temperature, and therefore, the problem is governed by non-linear parabolic equations. An implicit finite difference predictor-corrector procedure is used for numerical solution (Ames, 1992; Pacheco, 1994).

Phase transformation problem—Volumetric fraction of martensitic phase is determined in this problem. Evolution equations are integrated from a simple implicit Euler method (Ames, 1992; Nakamura, 1993).

Thermo-elastic problem—Stress and displacement fields are evaluated from temperature distribution. Numerical solution is obtained employing a shooting method procedure (Ames, 1992; Nakamura, 1993).

Elastoplastic problem—Stress and strain fields are determined considering the plastic strain evolution in the process. Numerical solution is based on the classical return mapping algorithm (Simo and Miehe, 1992; Simo and Hughes, 1998).

4. Numerical simulation

As an application of the general proposed model, numerical investigations associated with quenching of long steel cylindrical bar are carried out simulating a progressive induction (PI) hardening. This heat treatment process is carried out by moving a workpiece at a constant speed through a coil and a cooling ring. Applying an alternating current to the coil, a magnetic field is generated inducing eddy currents that heat the workpiece. When heated, a thin surface layer of austenite is formed. Afterward, a cooling fluid is sprayed on the surface by the cooling ring promoting the quenching of the layer, which is transformed into martensite, pearlite, bainite and proeutectoid ferrite/cementite depending on, among other things, the cooling rate. A hard surface layer with high compressive residual stresses, combined with a tough core with tensile residual stresses, is obtained.

This article considers PI hardening simulations in a cylindrical bar with radius R and a thickness of induced layer, e_{PI}. In order to consider the restriction associated with adjacent regions of the heated region, which are at lower temperatures, a plane strain state is adopted. Moreover, longitudinal heat conduction is neglected. Experimental results, obtained for similar conditions (Pacheco et al., 2001; Camarão, 1998), show that the proposed model captures the general behavior of experimental data.

Table 1
Material parameters (SAE 4140H)

$k = 1.100 \times 10^{-2}\ \mathrm{K}^{-1}$	$\kappa = 5.200 \times 10^{-11}\ \mathrm{Pa}^{-1}$	$M_s = 748\ \mathrm{K}$
$\gamma = 1.110 \times 10^{-2}$	$\rho = 7.800 \times 10^{3}\ \mathrm{kg/m^3}$	$M_f = 573\ \mathrm{K}$

Material parameters of SAE 4140H cylinder are presented in Table 1 and the latent heat released, associated with enthalpy change for austenite–martensite trasformation, is $\Delta H_m = 640 \times 10^6\ \mathrm{J/m^3}$. Other parameters depend on temperature and are interpolated from experimental data as follows (Melander, 1985; Hildenwall, 1979; Camarão, 1998; Pacheco et al., 2001; Silva, 2002):

$$E = E_A(1-\beta) + E_M\beta \begin{cases} E_A = 1.985 \times 10^{11} - 4.462 \times 10^7 T - 9.909 \times 10^4 T^2 - 2.059 T^3 \\ E_M = 2.145 \times 10^{11} - 3.097 \times 10^7 T - 9.208 \times 10^4 T^2 - 2.797 T^3 \end{cases} \tag{34}$$

$$H = \begin{cases} 2.092 \times 10^6 + 3.833 \times 10^5 T - 3.459 \times 10^2 T^2, & \text{if } T \leqslant 723\ \mathrm{K} \\ 2.259 \times 10^9 - 2.988 \times 10^6 T, & \text{if } 723\ \mathrm{K} < T \leqslant 748\ \mathrm{K} \\ 5.064 \times 10^7 - 3.492 \times 10^4 T, & \text{if } T > 748\ \mathrm{K} \end{cases} \tag{35}$$

$$\sigma_Y = \begin{cases} 7.520 \times 10^8 + 2.370 \times 10^5 T - 5.995 \times 10^2 T^2, & \text{if } T \leqslant 723\ \mathrm{K} \\ 1.598 \times 10^{10} - 2.126 \times 10^7 T, & \text{if } 723\ \mathrm{K} < T \leqslant 748\ \mathrm{K} \\ 1.595 \times 10^8 - 1.094 \times 10^5 T, & \text{if } T > 748\ \mathrm{K} \end{cases} \tag{36}$$

$$\alpha_T = \begin{cases} 1.115 \times 10^{-5} + 1.918 \times 10^{-8} T - 8.798 \times 10^{-11} T^2 + 2.043 \times 10^{-13} T^3, & \text{if } T \leqslant 748\ \mathrm{K} \\ 2.230 \times 10^{-5}, & \text{if } T > 748\ \mathrm{K} \end{cases} \tag{37}$$

$$c = 2.159 \times 10^2 + 0.548 T \tag{38}$$

$$\Lambda = 5.223 + 1.318 \times 10^{-2} T \tag{39}$$

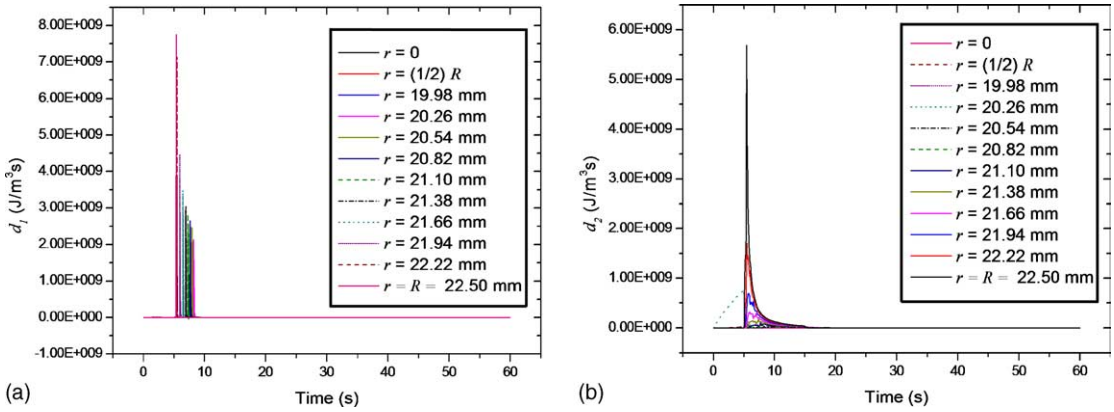

Fig. 2. Time history of dissipation. (a) Mechanical, d_1; (b) thermal, d_2.

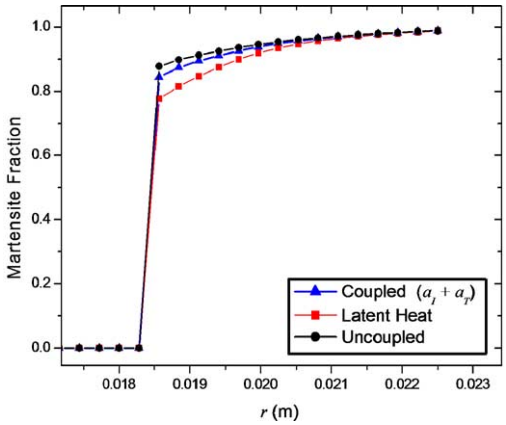

Fig. 3. Effect of thermo-mechanical coupling terms in the distribution of volumetric fractions of martensite through the radius.

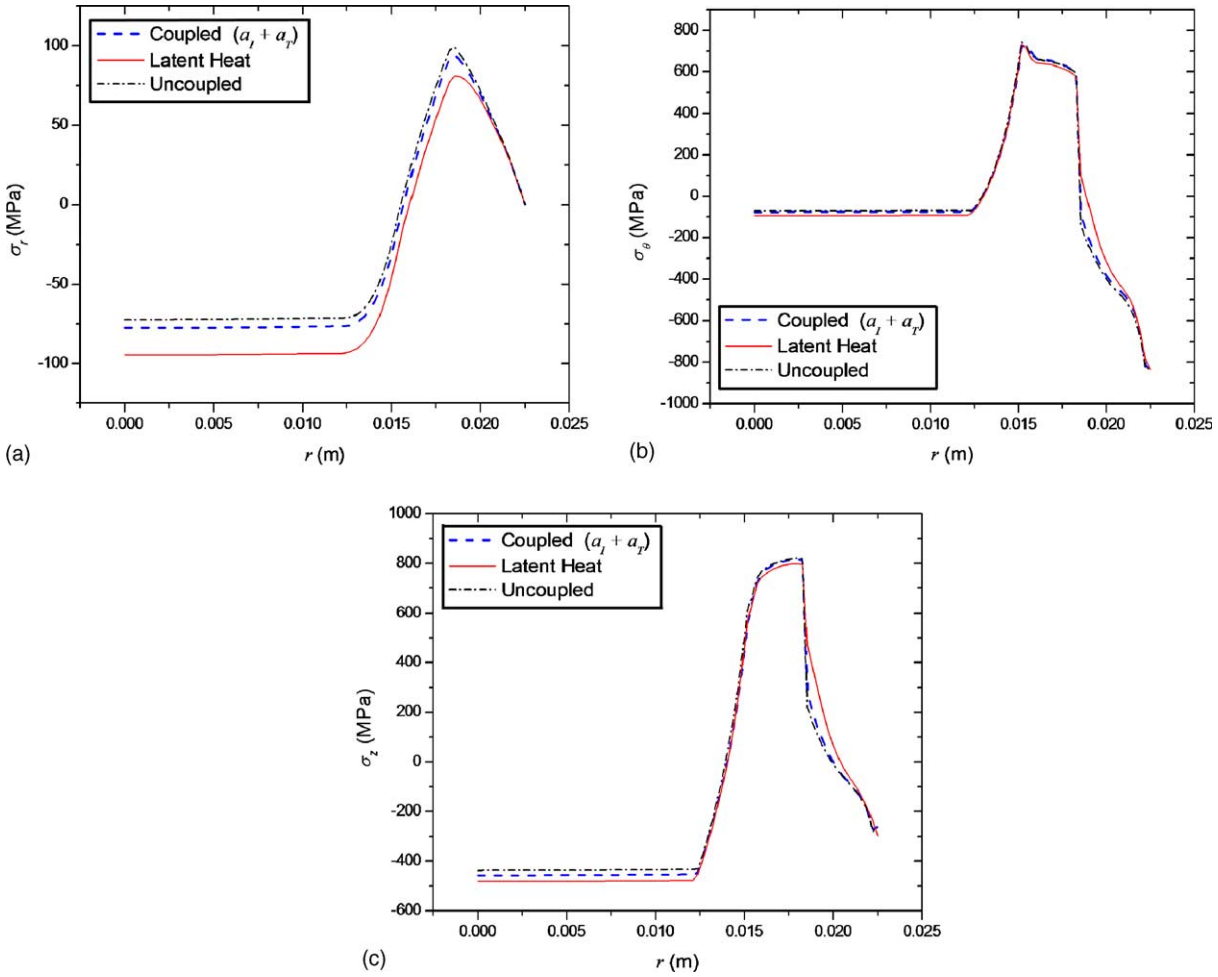

Fig. 4. Effect of thermo-mechanical coupling terms on the distribution of residual stress components. (a) σ_r; (b) σ_θ; (c) σ_z.

$$h_{\text{fluid}} = \begin{cases} 6.960 \times 10^{2}, & \text{if } T \leqslant 404 \text{ K} \\ 2.182 \times 10^{4} - 1.030 \times 10^{2} T + 1.256 \times 10^{-1} T^{2}, & \text{if } 404 \text{ K} < T \leqslant 504 \text{ K} \\ -2.593 \times 10^{4} + 5.500 \times 10^{2} T, & \text{if } 504 \text{ K} < T \leqslant 554 \text{ K} \\ -9.437 \times 10^{4} + 4.715 \times 10^{2} T - 7.286 \times 10^{-1} T^{2} + 3.607 \times 10^{-4} T^{3}, & \text{if } 554 \text{ K} < T \leqslant 804 \text{ K} \\ 1.210 \times 10^{3}, & \text{if } T > 804 \text{ K} \end{cases} \tag{40}$$

$$h_{\text{air}} = \begin{cases} 2.916 + 6.104 \times 10^{-2} T - 1.213 \times 10^{-4} T^{2}, & \text{if } T \leqslant 533 \text{ K} \\ 6.832 + 1.837 \times 10^{-2} T - 1.681 \times 10^{-5} T^{2} + 6.764 \times 10^{-9} T^{3}, & \text{if } 533 \text{ K} < T \leqslant 1200 \text{ K} \\ 3.907 \times 10^{1} - 2.619 \times 10^{-2} T, & \text{if } 1200 \text{ K} < T \leqslant 1311 \text{ K} \\ -2.305 \times 10^{1} + 3.366 \times 10^{-2} T, & \text{if } T > 1311 \text{ K} \end{cases} \tag{41}$$

where h is the heat convection coefficient.

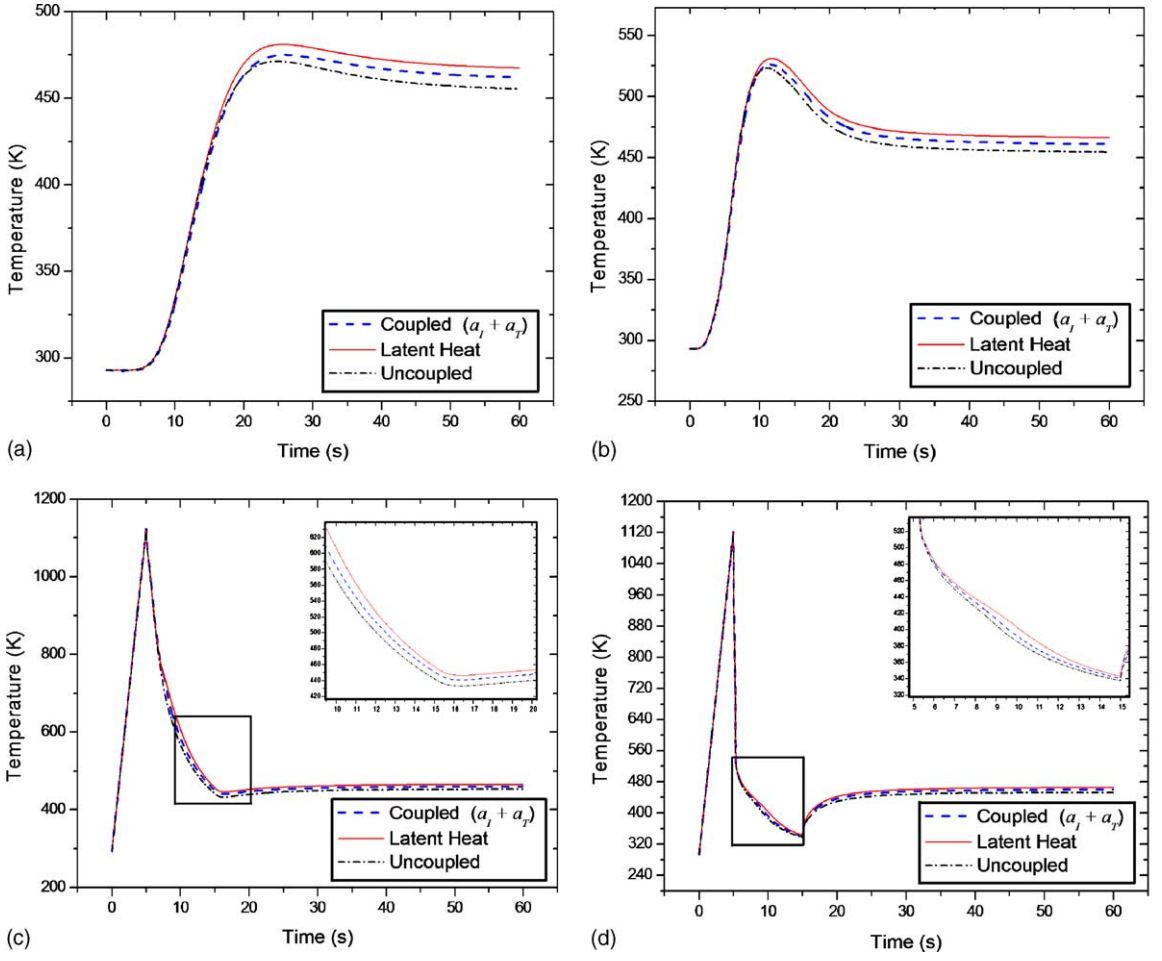

Fig. 5. Effect of thermo-mechanical coupling terms on the temperature distribution. (a) Center, $r = 0$; (b) $r = R/2$; (c) $r = 17.5$ mm; (d) surface, $r = R$.

The analysis of thermo-mechanical coupling starts considering a cylindrical bar with radius $R = 22.5$ mm. PI hardening simulations are developed considering a 3.5 mm thickness layer which is heated to 1120 K (850 °C) for 5 s and then sprayed by a liquid medium at 294 K (21 °C) for 10 s. Afterwards, air-cooling is assumed until a time instant of 60 s is reached. A convergence analysis is developed and a spatial discretization of 81 points with a variable time step (5.6×10^{-6} s for $t < 5$ s, 5.6×10^{-4} s for 5 s $\leqslant t < 15$ s and 5.0×10^{-2} s for $t \geqslant 15$ s) is adopted.

At first, dissipation terms related to the Clausius–Duhen inequality, d_1 and d_2 are analyzed. Fig. 2 presents the evolution of mechanical (d_1) and thermal (d_2) dissipation, for different positions in the cylinder considering the *coupled* model. It is clear that second law of thermodynamics is not violated since d_1 and d_2 values are always positive.

Martensitic volumetric fraction distribution through the radius is now considered for the final time instant. Different approaches to evaluate thermo-mechanical coupling terms are concerned in order to establish a comparison among results. *Latent heat* approach presents more drastically discrepancies than the proposed *coupled* model, when compared to results of *uncoupled* model (Fig. 3).

The forthcoming analysis presents residual stress components distribution for the final time instant. Results confirm the previous analysis for the volumetric fraction of martensite, showing that the consideration of the energy equation thermo-mechanical coupling terms (*coupled* model) in the analysis produce intermediate results between *uncoupled* analysis and the *latent heat* approach. Fig. 4 presents residual stress components distributions through the radius.

Temperature distribution is now focused. Fig. 5 presents the temperature time history for different positions in the cylinder. The energy equation thermo-mechanical coupling terms introduce a delay in the temperature evolution. In spite of the small amount, the delay can influence considerable diffusive phase transformations, for example, as pointed by Woodard et al. (1999).

Effects of energy equation thermo-mechanical coupling terms may become more pronounced for other geometry or quenching conditions. As examples, one could mention the thickness of the induced layer and the diameter of the cylinder. Woodard et al. (1999) exploit this second situation. The forthcoming analysis is concerned with situations that elucidate this behavior. At first, consider the previous example, related to a cylindrical bar with $R = 22.5$ mm. Fig. 6 shows values of circumferential and longitudinal residual stress

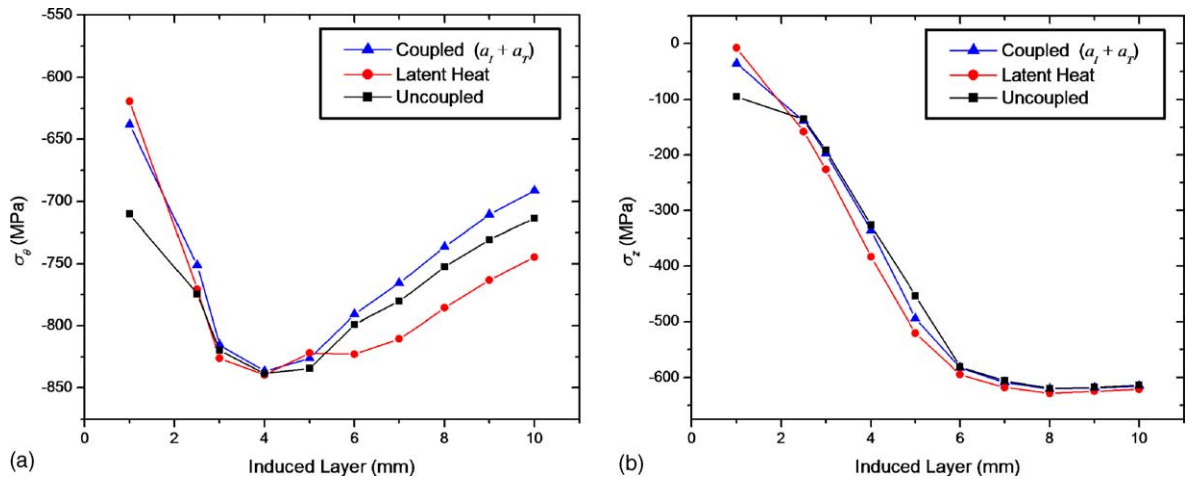

Fig. 6. Effect of thermo-mechanical coupling terms for different thickness of induced layer on stress components at the surface of a cylinder with $R = 22.5$ mm. (a) σ_θ; (b) σ_z.

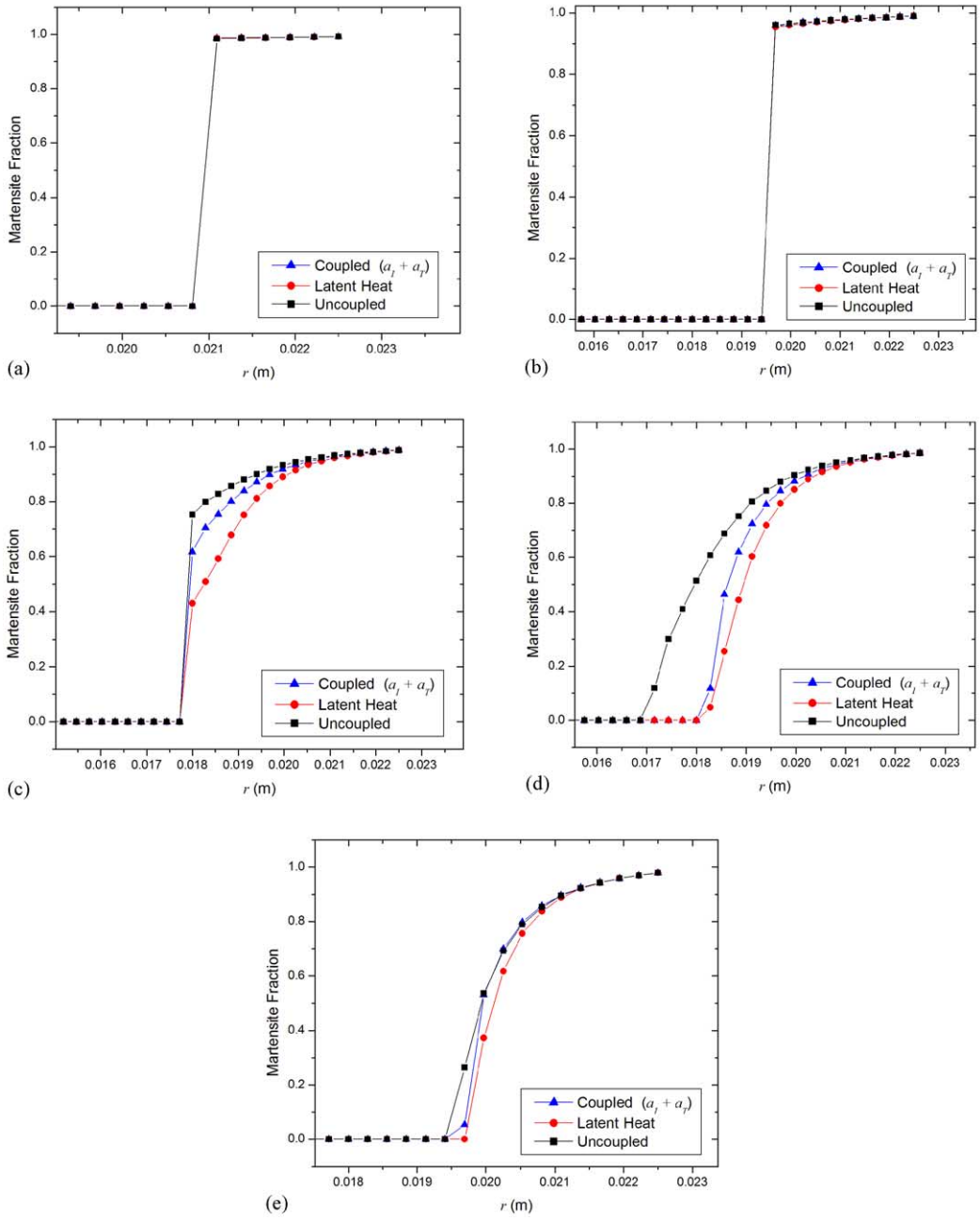

Fig. 7. Effect of thermo-mechanical coupling terms for different thickness of induced layer on the volumetric fractions of martensite in a cylinder with $R = 22.5$ mm. (a) 1 mm; (b) 2.5 mm; (c) 4 mm; (d) 5 mm; (e) 15 mm.

components at the surface of the cylinder for different thickness of induced layer. Notice that the effect of energy equation thermo-mechanical coupling terms is more pronounced for the smaller thickness value of induced layer. Assuming the *uncoupled* model as a reference, the *coupled* model presents a difference of

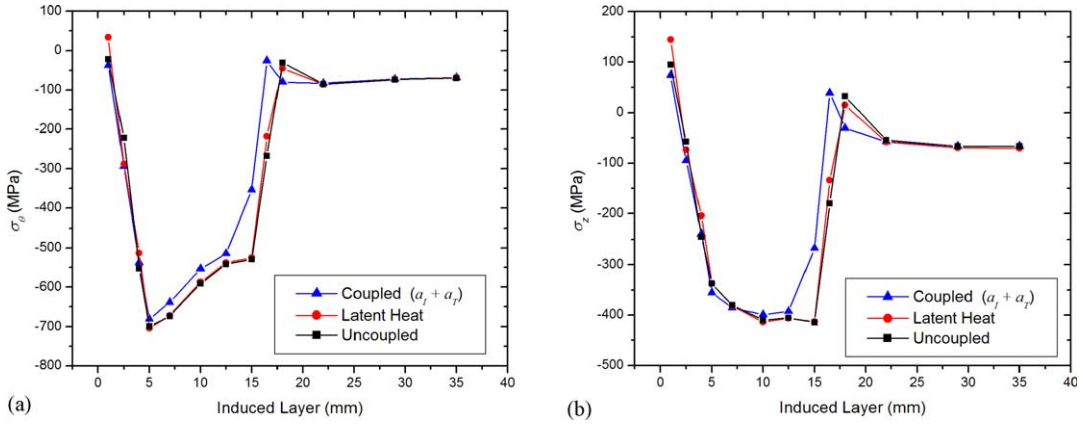

Fig. 8. Effect of thermo-mechanical coupling terms for different thickness of induced layer on stress components at the surface of a cylinder with $R = 100.0$ mm. (a) σ_θ; (b) σ_z.

about 70 MPa (10%) and 60 MPa (62%) for circumferential and longitudinal stresses, respectively. The *latent heat* approach present higher differences: 90 MPa for both circumferential and longitudinal stresses, meaning differences of 13% and 90%, respectively.

Fig. 7 shows that the effect of thermo-mechanical coupling terms related to the *coupled* and *latent heat* models become more important in martensitic volumetric fractions determination for intermediary values of the thickness of induced layer (5 mm).

At this point, a cylinder of radius $R = 100$ mm is considered. Under this situation, the effects of thermo-mechanical coupling terms are even more pronounced, confirming the conclusion of Woodard et al. (1999). Fig. 8 shows values for circumferential and longitudinal residual stress components at the surface of the cylinder for different thickness of induced layer. Considering the smaller thickness value of induced layer ($e_{\mathrm{PI}} = 1$ mm) and assuming the *uncoupled* model as a reference, differences of about 70% and 250% are observed for circumferential stress considering the *coupled* and *latent heat* models, respectively. On the other hand, using the same analysis for longitudinal stress, it is observed differences of about 20% and 50% considering the *coupled* and *latent heat* models, respectively. For e_{PI} values in the range of 15–18 mm, discrepancies among the *coupled* model with respect to the others is about 200 MPa for circumferential and 140 MPa for longitudinal stresses. For e_{PI} values greater than 22 mm, the three models present similar values of residual stresses.

Fig. 9 presents the distribution of matensitic volumetric fractions predicted by each model. Once again, for martensitic phase distribution, energy equation thermo-mechanical coupling terms become more important for a range of intermediary values of the thickness of induced layer (2.5–5 mm). For e_{PI} values greater than 12.5 mm, both *coupled* and *latent heat* models present similar martensitic phase distribution.

Fig. 10 shows the surface temperature evolution for the three models considering the same thickness of induced layer ($e_{\mathrm{PI}} = 1$ mm) and two different cylinder diameters ($R = 22.5$ and 100 mm). Notice that results predicted by *coupled* and *latent heat* models presents a small temperature jump at the cylinder surface due to the phase transformation. This behavior is more pronounced when cylinder diameter is increased.

5. Conclusions

The present contribution considers modeling and simulation of the quenching process, presenting an anisothermal model formulated within the framework of continuum mechanics and the thermodynamics of

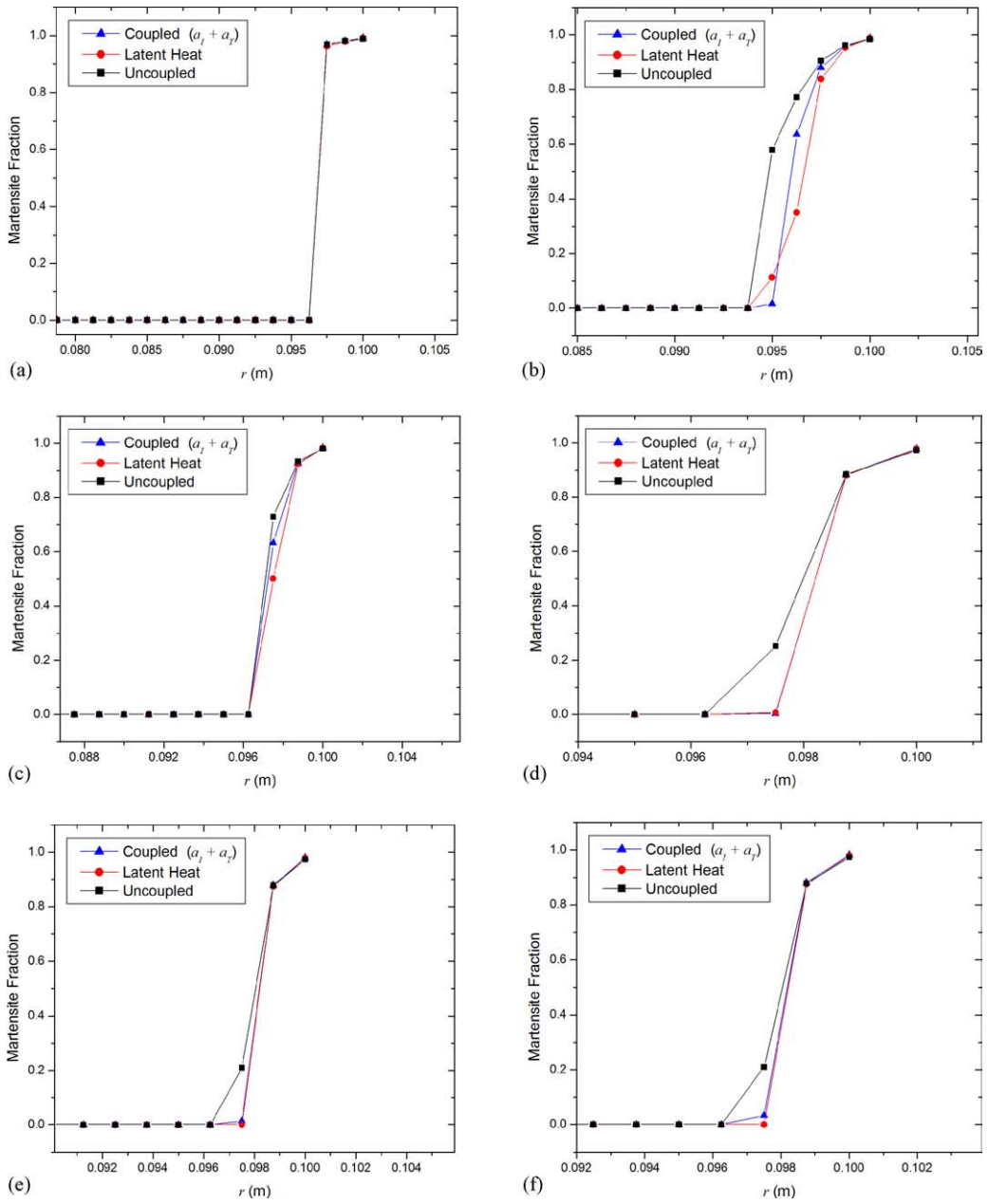

Fig. 9. Effect of thermo-mechanical coupling terms for different thickness of induced layer on the volumetric fractions of martensite in a cylinder with $R = 100.0$ mm. (a) 1 mm; (b) 2.5 mm; (c) 5 mm; (d) 12.5 mm; (e) 22 mm; (f) 35 mm.

irreversible processes. Progressive induction hardening of a cylindrical body is considered as an application of the proposed general formulation. Thermo-mechanical coupling is exploited in order to evaluate the effect of internal and thermal coupling terms in the energy equation. Three different models are considered with this aim: *Uncoupled*, which does not include energy equation coupling terms; *Latent heat*, with a source

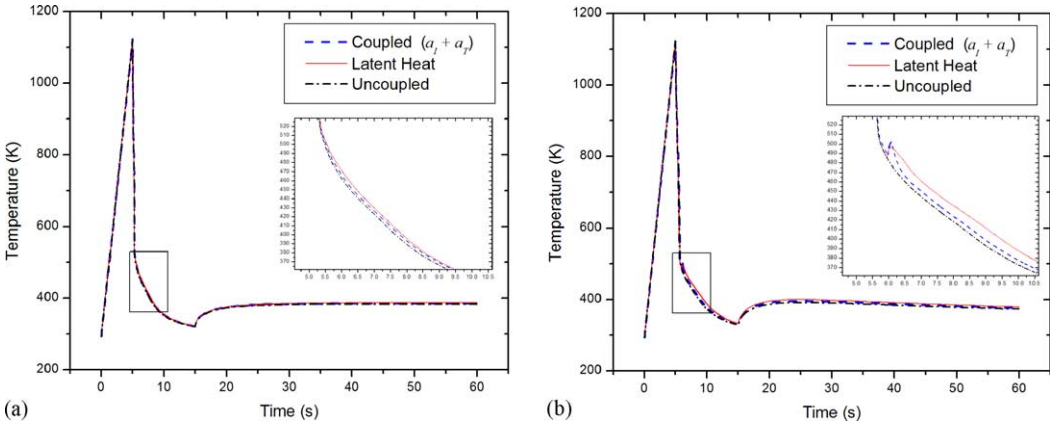

Fig. 10. Effect of thermo-mechanical coupling terms on the surface temperature distribution with $e_{PI} = 1$ mm. (a) $R = 22.5$ mm; (b) $R = 100$ mm.

term in the energy equation associated with the latent heat released during the martensitic phase transformation; and *Coupled*, that considers all coupling terms in the proposed model. Numerical simulations show that the energy equation thermo-mechanical coupling terms influence the determination of residual stress and the austenite–martesite phase transformation. These effects tend to become more pronounced in the analysis when greater diameters are considered. The variation of the thickness of induced layers related to progressive induced hardening is also an important parameter that influences the coupling terms. It should be pointed out that more drastically discrepancies may be expected in the analysis of quenching process considering other phases. Regarding temperature distribution, for example, even in situations where values are not considerably affected by the thermo-mechanical coupling terms, small temperature variations may cause different predictions for diffusive phase transformations because the time delay of the response. Besides, for the possibility of the formation of other phases (ferrite, pearlite and bainite) the proposed model predicts the incorporation of other coupling terms associated with these phases. Therefore, the authors agree that a complete comprehension of thermo-mechanical coupling terms must be obtained from the analysis of a model that contemplates diffusive and non-diffusive phase transformations.

Acknowledgements

The authors acknowledge the support of the Brazilian Agencies CNPq and CAPES.

References

Ames, W.F., 1992. Numerical Methods for Partial Differential Equations, 3rd ed. Academic Press.

Camarão, A.F., 1998. A Model to Predict Residual Stresses in the Progressive Induced Quenching of Steel Cylinders, Ph.D. Thesis, Department of Metallurgical and Materials Engineering, Universidade de São Paulo (in Portuguese).

Camarão, A.F., da Silva, P.S.C.P., Pacheco, P.M.C.L., 2000. Finite Element Modeling of Thermal and Residual Stresses Induced by Steel Quenching, In Seminário de Fratura, Desgaste e Fadiga de Componentes Automobilísticos, Brazilian Society of Automotive Engineering, Rio de Janeiro (in Portuguese).

Cherkaoui, M., 2002. Transformation induced plasticity: mechanisms and modeling. Journal of Engineering Materials and Technology 124, 55–61.

Denis, S., 1996. Considering stress-phase transformation interaction in the calculation of heat treatment residual stresses. Journal de Physique IV 6, 159–174.

Denis, S., Gautier, E., Simon, A., Beck, G., 1985. Stress-phase-transformation interactions—basic principles, modelling and calculation of internal stresses. Material Science and Technology 1, 805–814.

Denis, S., Sjöström, S., Simon, A., 1987. Coupled temperature, stress, phase transformation calculation model numerical illustration of the internal stresses evolution during cooling of a eutectoid carbon steel cylinder. Metallurgical Transactions A 18A, 1203–1212.

Denis, S., Farias, D., Simon, A., 1992. Mathematical model coupling phase transformation and temperature evolutions in steels. ISIJ International 32 (3), 316–326.

Denis, S., Archambault, S., Aubry, C., Mey, A., Louin, J.C., Simon, A., 1999. Modelling of phase transformation kinetics in steels and coupling with heat treatment residual stress predictions. Journal de Physique IV 9, 323–332.

Eringen, A.C., 1967. Mechanics of Continua. John Wiley, New York.

Fernandes, M.B., Denis, S., Simon, A., 1985. Mathematical model coupling phase transformation and temperature evolution during quenching of steels. Materials Science and Technology 1, 838–844.

Fernandes, M.B., Denis, S., Simon, A., 1986. Prévision de l'évolution Thermique et Structurale des Aciers au Cours de leur refroidissement Continu. Mémoires et Etudes Scientifiques Revue de Métallurgie, pp. 355–366.

Habraken, A.M., Bourdouxhe, M., 1992. Coupled thermo-mechanical-metallurgical analysis during the cooling process of steel pieces. European Journal of Mechanics A—Solids 11 (3), 381–402.

Hildenwall, B., 1979. Prediction of the Residual Stresses Created During Quenching. Ph.D. Thesis, Linkoping University.

Idesman, A.V., Levitas, V.I., Stein, E., 1997. Simulation of martensitic phase transition progress with continuous and discontinuous displacements at the interface. Computational and Materials Science 9 (1–2), 64–75.

Idesman, A.V., Levitas, V.I., Stein, E., 2000. Structural changes in elastoplastic materials: a unified finite-element approach to phase transformation, twinning and fracture. International Journal of Plasticity 18 (7–8), 893–949.

Koistinen, D.P., Marburger, R.E., 1959. A general equation prescribing the extent of the austenite–martensite transformation in pure iron–carbon alloys and plain carbon steels. Acta Metallurgica 7, 59–60.

Lemaitre, J., Chaboche, J.L., 1990. Mechanics of Solid Materials. Cambridge Press.

Levitas, V.I., 1997. Phase transitions in elastoplastic materials: continuum thermomechanical theory and examples of control—Part I and II. Journal of Mechanics and Physics Solids 45 (6), 923–947, 45(7) 1203–1222.

Levitas, V.I., 1998. Thermomechanical theory of martensitic phase transformations in inelastic materials. International Journal of Solids and Structures 35 (9–10), 889–940.

Levitas, V.I., 2000. Structural changes without stable intermediate state in inelastic material—Part I and II. International Journal of Plasticity 18 (7–8), 805–849, 851–892.

Melander, M., 1985. A Computational and Experimental Investigation of Induction and Laser Hardening, Ph.D. Thesis, Department of Mechanical Engineering, Linkoping University.

Nakamura, S., 1993. Applied Numerical Methods in C. Prentice-Hall, Englewood Cliffs, NJ.

Ortiz, M., Pinsky, P.M., Taylor, R.L., 1983. Operator split methods for the numerical solution of the elastoplastic dynamic problem. Computer Methods of Applied Mechanics and Engineering 39, 137–157.

Pacheco, P.M.C.L., 1994. Analysis of the Thermomechanical Coupling in Elastoviscoplastic Materials, Ph.D. Thesis, Department of Mechanical Engineering, Pontifícia Universidade Católica do Rio de Janeiro (in Portuguese).

Pacheco, P.M.C.L., Oliveira, S.A., Camarão, A.F., Savi, M.A., 1997. A model to predict residual stresses introduced by the quenching process in steels. In: Proceedings of the XIV Brazilian Congress of Mechanical Engineering—ABCM (in Portuguese).

Pacheco, P.M.C.L., Savi, M.A., Camarão, A.F., 2001. Analysis of residual stresses generated by progressive induction hardening of steel cylinders. Journal of Strain Analysis for Engineering Design 36 (5), 507–516.

Rockafellar, R.T., 1970. Convex Analysis. Princeton Press.

Sen, S., Aksakal, B., Ozel, A., 2000. Transient and residual thermal stresses in quenched cylindrical bodies. International Journal of Mechanical Sciences 42, 2013–2029.

Silva, E.P, 2002. Modeling and Simulation of Quenching Process in Steels using the Finite Element Method, M.Sc. Thesis, Department of Mechanical and Materials Engineering, Instituto Militar de Engenharia, October (in Portuguese).

Simo, J.C., Hughes, T.J.R., 1998. Computational Inelasticity. Springer.

Simo, J.C., Miehe, C., 1992. Associative coupled thermoplasticity at finite strains: formulation, numerical analysis and implementation. Computer Methods in Applied Mechanics and Engineering 98, 41–104.

Sjöström, S., 1985. Interactions and constitutive models for calculating quench stresses in steel. Material Science and Technology 1, 823–829.

Sjöström, S., 1994. Physical, mathematical and numerical modelling for calculation of residual stresses: fundamentals and applications. In: Proceedings of the Fourth International Conference on Residual Stresses, June 8–10, Baltimore, USA.

Wang, H.G., Guan, Y.H., Chen, T.L., Zhang, J.T., 1997. A study of thermal stresses during laser quenching. Journal of Materials Processing Technology 63, 550–553.

Woodard, P.R., Chandrasekar, S., Yang, H.T.Y., 1999. Analysis of temperature and microstructure in the quenching of steel cylinders. Metallurgical and Materials Transactions B 30B, 815–822.